Available online at www.sciencedirect.com
SCIENCE DIRECT®
Polymer 44 (2003) 6013–6032
polymer
www.elsevier.com/locate/polymer

Toughenability of polymers

A.S. Argon*, R.E. Cohen

Department of Mechanical Engineering, Massachusetts Institute of Technology, Room 1-306, MIT 77 Massachusetts Avenue, Cambridge, MA 02139-4307, USA

Received 25 March 2003; received in revised form 7 April 2003; accepted 7 April 2003

Dedicated to Prof. Ian M. Ward on the occasion of his 75th birthday

Abstract

We demonstrate that all solid polymers are intrinsically brittle and will undergo a ductile to brittle fracture transition based on the nature of their bonding alone. The most effective way of avoiding a ductile to brittle transition is to reduce the plastic resistance to delay reaching the brittle strength which in unoriented polymers is governed by intrinsic cavitation. While a number of possibilities for this exist, the most widely used techniques involve incorporation of rubbery particles that can cavitate or rigid particles that can debond prior to plastic flow. In both approaches the continuous homo-polymer is transformed into a quasi-regular cellular solid that is much more capable of undergoing large local plastic flow by ligament stretching between cavitated particles and is less susceptible to the propagation of brittle cracks under the usual conditions of tensile straining. Under impact conditions, however, in a notched sample which concentrates the strain rate at the notch root, the plastic resistance of the stretching ligaments rises sharply due to two separate but related effects. First, by an increase in the shear modulus due to the high frequency nature of the Izod impact test to fracture, viewed as a quarter cycle oscillation, which directly elevates the flow resistance and second, by the further effect of increase due to the much increased plastic strain rate. At the notch root then, the plastically stretching and strain hardening ligaments are left with a much reduced capacity to strain further before the cavitation stress is reached. While rubber particle-modified polymers can still exhibit considerable toughening, rigid-particle-modified polymers suffer severely from clustering of rigid particles into super critical flaws that trigger brittle response, much like what is encountered in structural steels.

Based on their known mechanical response in neat form six, semi-crystalline polymers have been analyzed in detail to evaluate their potential for toughening under impact conditions. The results correlate very well with the experimental findings.

Keywords: Toughenability of polymers; Intrinsic brittleness; Limitations on toughening

1. Introduction

Many, and perhaps all polymers in unoriented form are intrinsically brittle solids and will behave as such at low temperatures and high strain rates, particularly in the presence of crack-like flaws and notches. Throughout the years the subject of toughening of polymers has received wide-spread attention in a large number of conferences and symposia and in numerous publications [1–5]. In the vast majority of cases the attention has been of an empirical nature, often involving reports of results of blending of various component polymers with other polymers or particles of compliant or stiff nature. In most instances such reports have lacked mechanistic insight and therefore had limited predictive value in generalization of findings to other systems.

In the present communication we will take a fundamental and mechanistic perspective based on the phenomenology of brittleness of solids and its alleviation in diverse polymers. Since many components of our approach are well known and have been extensively developed our presentation will in part be brief.

2. Flaw-free inelastic deformation and fracture of polymers

2.1. Kinetics of plastic flow of polymers

The phenomenological and mechanistic aspects of large strain plastic deformation of both glassy and semi-crystalline polymers have been extensively explored. For overviews of a selection of these numerous developments see Refs. [6,7].

In glassy polymers the molecular level kinematics of the

* Corresponding author. Tel.: +1-617-253-2217; fax: +1-617-258-8742.
E-mail address: argon@mit.edu (A.S. Argon).

0032-3861/03/$ - see front matter © 2003 Elsevier Ltd. All rights reserved.
doi:10.1016/S0032-3861(03)00546-9

Nomenclature

E	Young's modulus
F	Izod impact striker force
G_{Ic}	critical energy release rate
J	J-integral work of fracture
J_e	essential work of fracture
K	strain hardening rate coefficient
K_B	bulk modulus
K_{Ic}	critical fracture toughness
K_c	bulk modulus of matrix
K_p	bulk modulus of particle
L	half length of Izod bar
M_c	entanglement molecular weight
R	universal gas constant
T	absolute temperature
T_{BD}	brittle to ductile transition temperature
Y_e	equivalent tensile plastic resistance of filled composite
Y_I	yield strength at Izod bar frequency
Y_0	yield strength in quasi-static tension experiment
a	crack length, notch depth
b	DCB specimen width
c	$= b - a$
d	particle diameter
h	Izod bar depth
k	Boltzmann's constant
m	phenomenological stress exponent of strain rate
n	phenomenological stress exponent strain hardening
p	thermal misfit clamping pressure on particles
r	radial coordinate
s	deviatoric stress at crack tip
v	striker velocity
Λ	interparticle ligament thickness
α	coefficient for ideal shear strength
β	coefficient for ideal cavitation strength
γ_c	volumetric coefficient of expansion of polymer matrix
γ_p	volumetric coefficient of expansion of particle
$\dot{\gamma}$	plastic shear strain rate
δ	terminal bending displacement of Izod bar
ε_0	strain at yield
ε_{f0}	strain to fracture in tension
ε_f	strain to fracture in impact
$\dot{\varepsilon}$	tensile plastic strain rate
ϕ	particle volume fraction
λ_1	uniaxial extension ratio
λ_n	locking sketch
ρ	material density, notch tip radius of curvature
μ_0	1 c/s shear modulus
$\mu_0(0)$	1 c/s shear modulus at $T = 0$ K
μ_I	shear modulus at Izod bar frequency
σ	shear stress in rate expression, otherwise applied stress
σ_B	tensile brittle strength
σ_e	equivalent (deviatoric) tensile stress
σ_m	mean normal stress
σ_∞	distant applied stress
$\tilde{\sigma}_e(\theta)$, $\tilde{\sigma}_m(\theta)$, $\tilde{\sigma}_{rr}(\theta)$, $\tilde{\sigma}_{\theta\theta}(\theta)$	angle-dependent dimensionless stress coefficients

deformation involves primarily rotational rearrangements among a large cluster of molecular segments resulting in a transformation shear strain of the order of 0.02 in volume elements of the order of 10 nm diameter where a small segmental, sub-set, as a core group, apparently acts as a thermally assisted trigger that releases the larger rearrangement [8,9]. Very satisfactory quantitative mechanism-based phenomenological rendering of the response has been provided earlier [10,11], and has proved to be highly accurate in computational modeling studies [12]. Once plastic flow is initiated through the repeated activation of such local shear transformations, in uniaxial extension they result in a progressive development of molecular orientation which bears a close correspondence to similar processes in the non-Gaussian stretching of elastomers having the characteristic temperature dependence of rubber elasticity [13]. The physical basis of this correspondence which relies on the ability of molecular conformational changes to sample phase space freely has been clarified only in recent experiments demonstrating that active plastic flow in glassy polymers sets up a 'flow-state' replicating the enhanced 'free' segment mobilities characteristic of those present at the glass transition temperature [14]. Here we represent this tensile plastic resistance σ merely in a symbolic form as:

$$\sigma = \hat{\tau}_1(T, \dot{\gamma}) + \rho \frac{RT}{M_c} f_2(\lambda_1, \lambda_n) \quad (1)$$

where in the first term on the RHS $\hat{\tau}$ represents the athermal plastic shear resistance (at 0 K) which is typically a substantial fraction of the shear modulus μ_0. A specific computer simulation for glassy polypropylene (PP) gives this value as $\hat{\tau} = 0.057\mu_0$ with $\mu_0 = 1.02$ GPa obtained by the same method [8,15]. In Eq. (1) $f_1(T, \dot{\gamma})$ represents a kinetic factor of the Arrhenian type giving the temperature and shear strain rate dependence of the plastic resistance. Moreover, in Eq. (1) the usual transformation between isotropic shear flow and isotropic tensile flow through the von-Mises formalism is invoked [16]. In the second term, on the RHS, $\rho RT/M_c$ made up of the density, universal gas constant, absolute temperature and the molecular weight between entanglements, represents the usual entropic rubbery modulus with f_2 representing, in turn, a Langevin type functional dependence that gives the strain hardening behavior based on the uniaxial extension ratio λ_1 and the locking stretch λ_n of the molecular network. We note here that the second term that represents the strain hardening behavior has a kinetic temperature dependence characteristic of rubber elasticity [13] and differs fundamentally from that of the first term which is Arrhenian.

In semi-crystalline polymers the large strain plastic flow is primarily of a crystal plasticity nature, involving mostly chain sliding on one or more crystallographic slip planes in the crystalline component of the polymers, produced by the passage of crystal dislocations. This deformation dominates the plastic response once the equivalent strain exceeds 10–15% during the initial phases of deformation where the response of the amorphous component is dominant, but 'locks-up' to require all subsequent deformation to be provided by the crystalline component [17]. Although the temperature and strain rate dependence of this deformation resistance is also known to be on an Arrhenian nature its precise mechanistic origin is still somewhat obscure. There is considerable support for a flow resistance mechanism based on thermally assisted overcoming of glide obstacles by screw dislocations in a quasi single crystalline material produced by plane strain compression and subsequently probed in simple shear [18]. In the usual melt-crystallized material with lamellar crystallites of thickness of 10 nm, however, it is likely that the rate process is governed by repeated nucleation of dislocations from interfaces between crystallites and amorphous layers [19]. As in glassy polymers, increasing plastic strain produces molecular orientation, but in this case by crystallographic shear-induced development of deformation texture as has been demonstrated by computer simulations in HDPE [20] and in other semi-crystalline polymers [21]. Although the stress–strain curves developed by such crystallographic shears closely resemble those of glassy polymers as shown in Fig. 1, the physical mechanisms are radically different with a consequence that the strain hardening behavior is no longer freely separable from the flow resistance as is the case in glassy polymers. Moreover, it has an Arrhenian temperature dependence linked to that of the crystallographic shear, amounting to an increase in resistance with decreasing temperature [24]. Apart from the more definitive simulations of the plastic deformation process in semi-crystalline

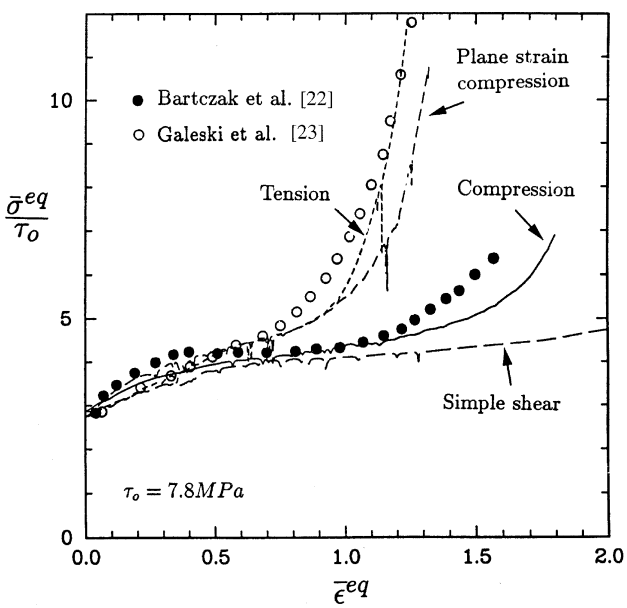

Fig. 1. Computed normalized equivalent stress vs. equivalent strain curves for tensile, compressive and shear deformation of HDPE, compared with experiments of Bartzak et al. on uniaxial compression [22] and Galeski et al. for plane strain compression [23] (from Lee et al. [20], courtesy of Elsevier).

polymers cited above, there are a large number of very useful experimental studies, a particular set of which due to G'Sell and Jonas will be referred to extensively in Section 9.2.

2.2. Ideal fracture of unoriented polymers

The toughness of polymers is governed by a competition between plastic deformation and a terminal process of fracture. While fracture is ultimately governed by cracks and notches that concentrate stresses and strains, the local process is one of the separation that must be understood as the response of the flaw-free polymer to a tensile stress or a negative pressure. Such an ideal response is best studied by a computational simulation as has been carried out by Mott et al. [25] on a molecular model of glassy PP subjected to increasing negative pressure. The results of this model are shown in Fig. 2 for three different cubic simulation cells ranging from edge dimensions of 1.815 to 2.615 nm to finally 3.396 nm, respectively. The figure shows the negative pressure response as a function of applied dilatation, compared with the prediction of a universal binding energy relation (UBER) due to Rose et al. [26] for a perfect solid having the same physical and elastic properties as the PP but containing no structural imperfections. The figure shows that as the system size increases the cavitation strength decreases and levels off at roughly 95 MPa for the largest system which represents a fraction of 0.028 of the bulk modulus of $K_B = 3.37$ GPa, determined by a similar computer simulation [15]. We consider this as an ideal response of a typical glassy polymer incorporating molecular level heterogeneities.

3. Flaws, cracks, notches and extrinsic heterogeneities

Most commercial polymer product contains various imperfections such as cracks, notches, and extrinsic heterogeneities where stresses are concentrated resulting in concentrations of strain and enhancement of strain rate, all of which localize the fracture process. The control or management of such flaws is a key to govern the fracture processes that limit material toughness. The forms of stress and strain concentration around such discontinuities or heterogeneities are well documented in the literature for elastic response around holes of various shapes and notches [27,28], around crack tips in a variety of settings [29,30], around crack tips in material exhibiting power-law hardening [31] and around crack tips in material obeying power-law creep [32].

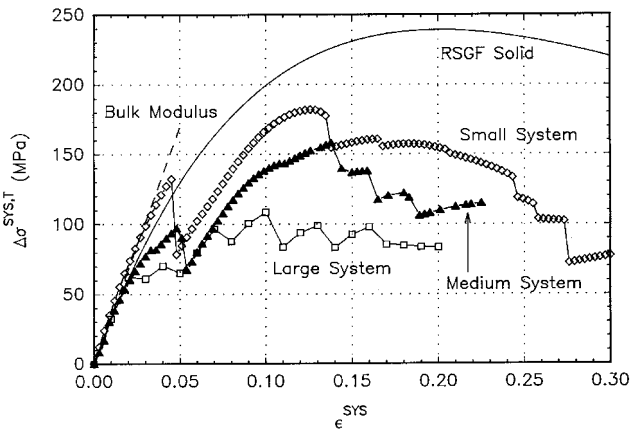

Fig. 2. Computed mean normal stress vs. dilatation curve for glassy polypropylene at 253 K, showing results for three sizes of simulation cells. The larger the cell, the more susceptible is the material to cavitation [25]. Results compared with predictions of the universal binding energy relation [26] (from Mott et al. [25], courtesy of Taylor & Francis). R.S.G.F. stands for the initials of the authors of Ref. [26].

4. Intrinsic brittleness or intrinsic toughness of polymers

In the consideration of toughening of polymers it is instructive to note at the outset that, most, if not all, unoriented polymers are intrinsically brittle solids in the definition of Kelly et al. [33], where a defining condition is considered at the tip of an atomically sharp crack subjected to Mode I loading across the plane of the crack. In such loading, all stresses are concentrated around the crack tip in a characteristic way given as

$$\sigma_{ij}(r,\theta) = \frac{K_I}{\sqrt{2\pi r}}\tilde{\sigma}_{ij}(\theta) \tag{2a}$$

$$K_I = \sigma_\infty\sqrt{\pi a} \tag{2b}$$

in the crack tip coordinate system shown in Fig. 3, where a, is the crack length, r and θ, the cylindrical coordinates, σ_∞, the distant applied tensile stress and $\tilde{\sigma}_{ij}(\theta)$, a definite θ dependent function [29]. Then, if in an otherwise flaw-free and homogeneous material the local shear stresses or deviatoric stresses, concentrated at the crack tip initiate plastic flow before the tensile stress or the negative pressure along the extension of the plane of the crack reaches the decohesion strength or the ideal cavitation strength of the solid, that solid is characterized as intrinsically ductile and is a candidate for tough response under even the most

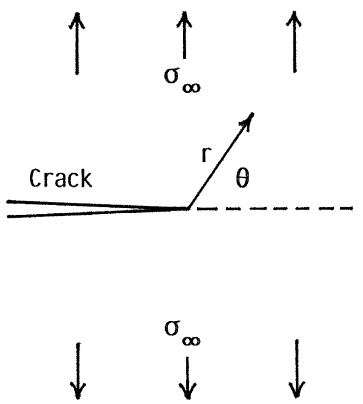

Fig. 3. Mode 1 crack field.

adverse conditions. On the other hand, if the opposite conditions hold, the solid is characterized as intrinsically brittle. It is an interesting observation that because of the character of bonding, with the exception of only a small class of pure metals all other solids are intrinsically brittle. (for a listing of solids separated in this fashion see Ref. [34]). This includes solid polymers. A clear demonstration of this fact is readily possible purely on a theoretical mechanistic basis.

Consider the case of amorphous polypropylene, the ideal plastic response and cavitation response of which was simulated in considerable detail [8,15,25] under pure shear deformation and under pure dilatation, respectively. As already stated in Sections 2.1 and 2.2 the otherwise ideal plastic shear resistance $\hat{\tau}$, and the ideal cavitation resistance $\hat{\sigma}$ were determined to be [8,25]:

$$\hat{\tau} = \alpha\mu_0 \tag{3a}$$

and

$$\hat{\sigma} = \beta K_B \tag{3b}$$

where μ_0 and K_B, the rate independent shear and bulk moduli that were obtained in a similar earlier simulation as [13]:

$$\mu_0 = 1.02\ \text{GPa} \tag{4a}$$

and

$$K_B = 3.37\ \text{GPa} \tag{4b}$$

respectively, with

$$\alpha = 0.057 \tag{5a}$$

and

$$\beta = 0.028 \tag{5b}$$

being the specific levels of the respective resistances.

However, in the Mode I field around an atomically sharp crack the concentration of the deviatoric shear stress s and the negative pressure σ_m are given as special cases of Eq. (2a) as:

$$\sigma_{m\ max} = \frac{K_I}{\sqrt{2\pi r}}\tilde{\sigma}_m(\theta = 0) \qquad (\tilde{\sigma}_m = 0.907) \tag{6a}$$

$$s_{max} = \frac{K_I}{\sqrt{2\pi r}}\tilde{s}(\theta = 108^\circ) \qquad (\tilde{s} = 0.396) \tag{6b}$$

where the maximum values of these local field intensities are concentrated at $\theta = 0$ at the extension of the crack plane for the mean normal stress and at $\theta = 108^\circ$ for the deviatoric shear stress, respectively. We note that since

$$\frac{\sigma_{m\ max}}{s_{max}} = 2.29\rangle 1.62 = \frac{\hat{\sigma}}{\hat{\tau}} \tag{7}$$

cavitation will be overwhelmingly preferred ahead of the crack, well before any plastic flow can be initiated from the crack tip. Thus, it must be concluded that in this special case, at least, the polymer polypropylene is intrinsically brittle on the basis of the criterion of Kelly et al. If we can take the simulations of Mott et al. [8,25] on PP as being broadly reflective of the behavior of other amorphous polymers, and by implication applicable to the amorphous components of even semi-crystalline polymers, and the coefficients α and β are applicable to other amorphous polymers as well, we can reach more definitive conclusions on intrinsic brittleness, provided for other such cases $\hat{\sigma}/\hat{\tau} = (\beta/\alpha)(K_B/\mu_0)$ is also less than 2.29 as required by Eq. (7). In Table 1 the key mechanical properties of six prominent semi-crystalline polymers are given where their K_B/μ_0 ratios are listed in column 6. Multiplication of these ratios with the ratio of $\beta/\alpha = 0.491$ gives the estimates of $\hat{\sigma}/\hat{\tau}$ to be all well below the critical ratio of 2.29.

This conclusion might also be sought by examining the fracture toughnesses K_{IC}, the critical fracture resistances at decreasing temperature. Unfortunately, here the information is incomplete and not well documented. The scattered available information indicates that in homopolymers ranging from epoxy resins (DGEBA) (0.7 MPa$\sqrt{m}$, at $-45\,^\circ$C) [35], to PC (2.1 MPa$\sqrt{m}$, at $-70\,^\circ$C) [36]; PMMA (1.4 MPa$\sqrt{m}$ at $-140\,^\circ$C) [37]; PS (0.9 MPa$\sqrt{m}$ at $-100\,^\circ$C) [37] and PE (2.4 MPa$\sqrt{m}$ at $-160\,^\circ$C) [37], these fracture toughnesses were under 2.4 MPa$\sqrt{m}$ and can at first sight be considered small. However, when converted to the specific work of fracture $G_{IC}(= K_{IC}^2(1-\nu^2)/E)$ they range from about 13.6 to 160 J/m^2 and are all very much larger than an estimated value of about 0.1 J/m^2 for twice the surface energy of these polymers and indicate that a considerable amount of dissipative fracture work has accompanied the measurements. In the only well documented case of PMMA and PS [38,39] the work of fracture G_{IC} rose systematically with decreasing temperature down to $-40\,^\circ$C, almost in direct proportion with the known increase in the plastic shear resistance of these glassy polymers with decreasing temperature. These two observations are fully consistent with the known fact that in both of these polymers cleavage-like fracture is preceded by the advance of a craze which is then split by the crack that follows, giving a fully quantitative accounting of the specific works of fracture. In none of these cases, however, accounting for the specific works of fracture were the measurements taken down to real cryogenic temperatures to fully test the theoretical predictions. In any event the reported fracture toughnesses of under 2.4 MPa$\sqrt{m}$ are too low to be of use for technological purposes and even with their definite accompanying plastic dissipation at the inception of crack growth this can be taken as evidence for brittle behavior.

5. Brittle to ductile transitions in fracture

Intrinsically brittle polymers together with other such solids exhibit a transition from brittle to tough behavior, since while their brittle strength σ_B, governed by microstructural

Table 1
Mechanical properties and plastic response characteristics of some semi-crystalline polymers

Polymer	μ_0 (MPa)	μ_1 (MPa)	K_B [a] (MPa)	T_g (K)	$K_B/\mu_0(0)$ [b]	$\beta K_B/\alpha\mu_0$	Y_0 [c] (MPa)	ρ [d] (g/cm^3)	$(d\sigma)/(d\ln\dot{\varepsilon})$ [c] (MPa)	$m = (d\ln\dot{\varepsilon})/(d\ln\sigma)$ [c]	$\Delta v_0^* (nm)^3$	$K = (1/3)(d\sigma/d\varepsilon)^c_{\varepsilon=0}$
PA-66 (Nylon- 66)	650[e]	1080[e]	6500	310[e]	2.55	1.252	103.0	1.24	1.55	66.5	2.67	16.8
PA-6 (Nylon-6)	650[e]	1080[e]	6450	310[e]	2.53	1.242	73.0	1.23	2.19	33.4	1.89	11.0
PVC	390[f]	655[f]	5180	358[d]	2.11	1.036	57.1	1.52	1.24	46.0	3.34	14.0
HDPE	660[g]	1660[g]	4540	195[d]	2.21	1.085	30.8	1.00	1.98	15.6	2.09	2.4
PP	880[g]	1780[g]	4370	263[d]	1.62	0.795	38.3	0.95	1.32	28.8	3.13	4.2
LDPE	200[g]	1000[g]	3300	195[g]	2.06	1.011	11.9	0.95	0.94	12.6	4.39	2.2

[a] Hartmann and Jarznski [80].
[b] Asymptotic values of $\mu_0(0)(T \to 0)$ were obtained from Schmieder and Wolf [85].
[c] G'Sell and Jonas [79].
[d] van Krevelen [84].
[e] Lin and Argon [18].
[f] Koleske and Wartman [83].
[g] McCrum et al. [82].

flaws or extrinsic imperfections, is relatively independent of temperature, their tensile plastic resistances Y_0 are far more temperature and strain rate dependent as discussed in Section 2.1. Thus a polymer that is brittle at low temperature can become tough above a certain transition temperature T_{BD} at a given strain rate $\dot{\varepsilon}$ as depicted in the well known Davidenkov construction [16] shown in Fig. 4(a). Increasing strain rate that evokes an increase in plastic resistance will result in an increase in T_{BD}. Once plastic response is initiated it will result often in amelioration of some of the microstructural imperfections that could trigger brittle behavior and eventually lead to molecular alignment or texture development that can significantly elevate the strength across the extension directions. As Fig. 4(b) shows, however, strain hardening also increases the deformation resistance even faster than the increase in strength, eventually resulting in fracture at a given plastic strain ε_f^p. Here too the strain-induced elevation of fracture stress or fracture resistance, is relatively independent of strain rate or temperature while the rising plastic resistance $Y(\varepsilon^p)$ is dependent on both. As Fig. 4(b) and (c) shows, the final fracture strain decreases with decreasing temperature and increasing strain rate.

Clearly, the homogeneous deformation response shown in Fig. 4 also applies in inhomogeneous flow where notches and other local strain concentrations are present. There, through the double effect of enhancement of the local strain hardening and strain rate global embrittlement will result.

6. Strategies for toughening

While synthesizing new polymers that are not intrinsically brittle, or increasing the microstructural perfection of those that are by improvements in processing to exclude flaws and inclusions is always an option to improve toughness, this is often either fundamentally not possible or technologically not profitable. In that case the only option available is to decrease the global plastic resistance to suppress the T_{BD} to lower temperatures. Most, if not all, approaches to toughening either deliberately or fortuitiously have followed this route, which when intelligently practiced can be very effective. In Section 7 we take an overview of the possibilities, some of which we consider in more detail later.

7. Options for toughening by reduction of plastic resistance

7.1. Glassy polymers

Some glassy polymers exhibit crazing as a distinct form of localized dilatational plastic flow, which has been studied in great detail. For summaries see Refs. [40,41]. While much has been clarified on crazability of glassy polymers,

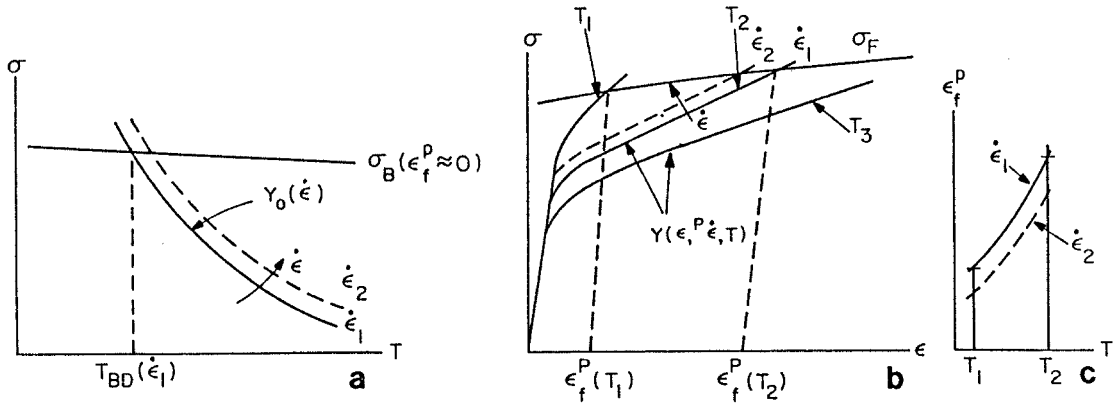

Fig. 4. Sketch of the well-known Davidenkov construction of a brittle to ductile fracture transition: (a) T_{BD} defined as the intersection of the brittle strength curve σ_B and the yield strength $Y_o(\dot\varepsilon)$ that depends on strain rate $\dot\varepsilon$; (b) reduction in the strain to fracture ε_f with increasing strain rate; and (c) with decreasing temperature at constant strain rate (from Argon et al. [86], courtesy of Riso NL, Denmark).

through its sensitivity to entanglement molecular weight [40] of flexible chain polymers, and other considerations have also been advanced based on the effectiveness of short range order in inflexible chain polymers to explain their craze resistance and other effects of craze suppression such as small increments of warm plastic pre-stretch [42], there is still no fully satisfactory understanding of the crazability of polymers. However, since fracture in crazable polymers is caused by craze matter fracture by either intrinsic processes of chain scission or by particulate heterogeneities that locally 'precipitate' this process, many effective procedures have been advanced to nurture toughening—all by the reduction of overall deformation resistance to avoid premature craze fracture. Apart from blending non-crazable polymers with crazable ones to increase the craze flow stress above the distortional plastic resistance [43], the majority of approaches to toughening crazable polymers such as PS have been based on the incorporation of compliant heterogeneities effective in increasing the craze concentration by promoting nucleation of crazes such as what happens in high-impact-polystyrene (HIPS) and other variants. The mechanistic aspects and mechanics of this approach are well developed and will not be explored further here [1,44–47]. A further approach to toughening by lowering the craze resistance through plasticization-on-demand by pre-packaged low molecular weight diluents has also been explored widely [48,50]. These, while quite effective in certain ranges have been ineffective at high strain rates because of the limitations of the stress enhanced processes of Case II diffusion which govern the local plasticization process [50–52]. Some of the fundamental limitations of this approach involving the deformation enhanced Case II diffusion have only recently been understood [14].

Since toughening of glassy thermoplastic polymers is not the primary direction of our present communication we will not develop this subject further.

7.2. Thermosetting polymers

Epoxies are used widely as matrix materials in polymer–matrix fiber-composites and other allied applications where they are used in more bulky forms. Hence, their brittleness has stimulated much development. Incorporation of compliant particles into epoxies to achieve parallel results to HIPS have basically failed [53] for fundamental reasons that such polymers are not crazable and also have high plastic resistances due to their molecular network architecture. Nevertheless, incorporation of well dispersed, micron-sized compliant particles have proved to be effective in promoting a mode of cavitational localization of the particles under stress [54] giving rise to a response akin to the cavitational craze process found in spherical-domain block copolymers [55] where the presence of thermal misfit stresses in the rubbery heterogeneities have been shown to play a prominent role. Since our principal assignment is to elucidate processes of toughening of semi-crystalline polymers by particulate heterogeneities, we will also not pursue further the case of thermosetting resins.

7.3. Semi-crystalline polymers

Many prominent semi-crystalline polymers such as high density polyethylene (HDPE), polyamides (PA, Nylon), and polypropylene (PP) are generally known to be quite tough in the usual forms of usage away from low temperatures and at moderate rates of deformation. However, they are also known to be notch-brittle, particularly at low temperatures and under impact loading. These polymers have been successfully toughened by incorporation of rubbery heterogeneities for some time. Much of the recent work on such polymers has been primarily on PA [56–63] and has emphasized in part the correlation between toughenability and the critical interparticle ligament dimension. The latter has been mechanistically related to a special form of

preferential crystallization around the particles that has been shown to reduce the overall plastic resistance of the polymer matrix [58,59]. Considerable work was carried out on isotactic polypropylene (iPP) using both rubbery [64,65] and stiff particles [66a,b,67]. Polyethylene was also studied in this sense with both rubbery and stiff particle modification [68,69] again through exploring the critical interparticle ligament effect. We will not review this work here but will rather concentrate on the principles that have been emerging from these extensive studies.

8. Toughening of semi-crystalline polymers by stiff particles

8.1. Motivation

By long standing practice, probably dating back to the introduction of high impact polystyrene (HIPS), toughening has usually been associated with incorporation of a rubbery component into the brittle polymer, perhaps on the argument that through a 'rule-of-mixture-thinking' the high elastic flexibility of rubber must mitigate brittleness in solid polymers. However, Kinloch [70] demonstrated that brittle epoxies can be toughened nearly as effectively by using either cavitating rubbery particles or by debonding glass spheres, indicating that the toughening mechanism has little to do with the mechanical properties of the particles but is governed by the debonding or cavitation process and works through the principle of crack tip shielding, often in more than one form [71]. Then, if the volume fractions and random dispersions of particles can be made comparable it should be more beneficial to use stiff particles since they would also improve elastic stiffness of the overall composite, roughly by as much as rubbery particles would compromise it. For this reason we will consider here only the effect of modification of brittle semi-crystalline polymers with stiff, equiaxed particles but also refer to corresponding practice with rubbery particles for comparison.

8.2. Changed elastic stiffness and plastic resistance due to stiff particles

The introduction of equiaxed particles of given elastic properties into a topologically continuous matrix has been analyzed by many authors, e.g. by Chow [72] using the Eshelby inclusion method [73]. Specific examples of such use with $CaCO_3$ particles in Nylon were recently presented [63]. Incorporation of such nearly rigid particles by typically a volume fraction of between 0.2 and 0.25 will elevate the shear modulus of the composite by roughly 60% and the bulk modulus by 35%. This compares well with a roughly similar magnitude reduction in these moduli if rubbery particles were introduced into the matrix polymer instead, illustrating the advantage of using stiff particles. It

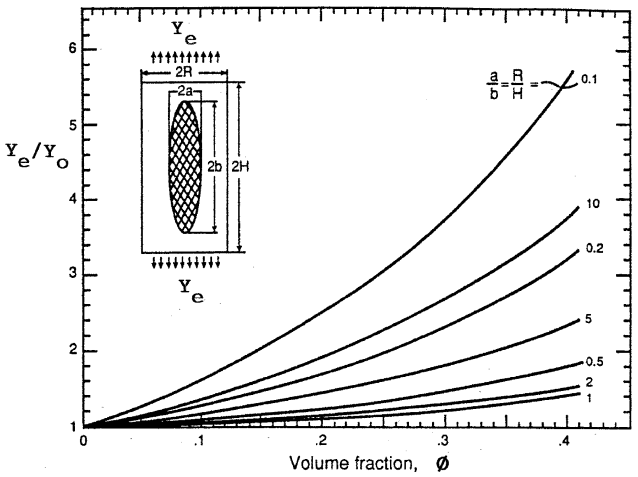

Fig. 5. Normalized equivalent tensile plastic resistance $Y_e(\phi)/Y_0$ as a function of volume fraction ϕ of rigid ellipsoidal filler particles (from Bao et al. [87], courtesy of Pergamon Press).

is useful to note that the changed elastic properties are dependent only on volume fraction and not on particle dispersion. There is also a corresponding effect on the tensile plastic resistance. Fig. 5 shows the effect on the tensile plastic resistance ratio Y_e/Y_0 resulting from the incorporation of non-deformable particles into a plastically deformable neat matrix with yield strength Y_0 with increasing volume fractions of rigid particles of different aspect ratio and aligned principal axes. As the figure shows, for equiaxed particles a volume fraction of 0.2–0.25 gives an increase of roughly 1.2 for perfectly adhered particles. Clearly, for the purpose of toughening where reduction in plastic resistance is required, rather than an increase, this would be undesirable and result in embrittlement. Thus, the need for debonding of rigid particles prior to yielding of the matrix. We present successful examples of this desirable behavior in HDPE Nylon and iPP in Section 8.3 below.

8.3. Reduction in plastic resistance upon introduction of debonding rigid particles

Incorporation of $CaCO_3$ particles of 0.7 μm diameter obtained by precipitation from solution, and coated with calcium stearate to achieve proper dispersion in polymer matrixes has been quite effective in controllably lowering the plastic resistance while achieving increases in small strain elastic properties, in HDPE [69]; PA-6 [63] and iPP [66a,b]. A successful case in PA-6 is shown in Fig. 6 giving the stress–strain curve of modified blends at room temperature for volume fractions up to 0.28 [63].

The clearly discernable kinks in the elastic portions of the stress–strain curves for the larger volume fractions demonstrate that the particles have debonded before overall yield, resulting in a systematic reduction of the tensile yield stresses which are shown further in Fig. 7 for two cases, involving in addition to the blends with 0.7 μm size particles also blends with 3.5 μm average size particles

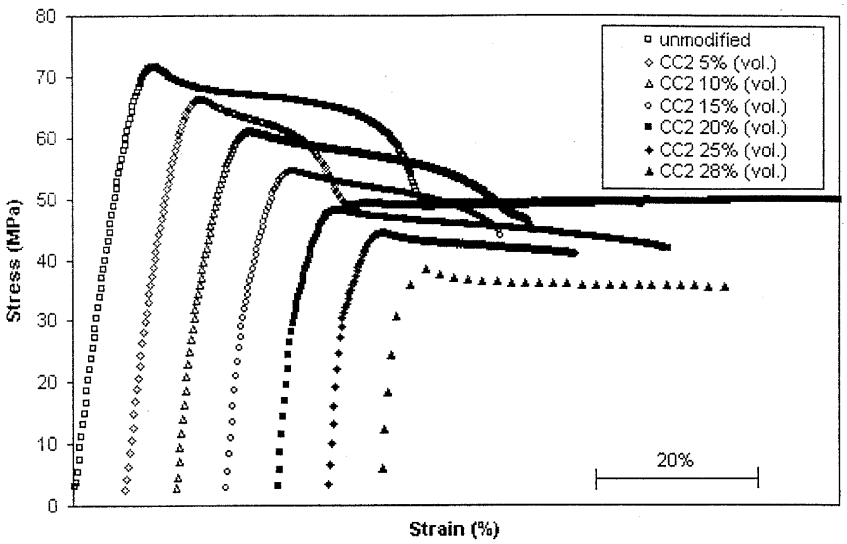

Fig. 6. Tensile engineering stress–strain curves of PA-6 modified with 0.7 μm diameter $CaCO_3$ particles with volume fractions up to 0.28. Note the kinks in the elastic loading lines where particle separation occurs. (from Wilbrink et al. [63], courtesy of Elsevier).

with, however, an undesirable wide particle size distribution. In both cases the trend in reduction in yield stress with increasing volume fraction ϕ is identical and falls under an upper bound estimate given by the solid line. The line going through the data has a form of $Y = Y_0(1 - 1.62\phi)$. A related finite element solution [74] represents a closer fit to the data. From similar stress–strain experiments carried out at different temperatures which demonstrated a systematic increase in the debonding stress with decreasing temperatures and a complete reversibility of the kinked elastic loading line behavior upon unloading and reloading,

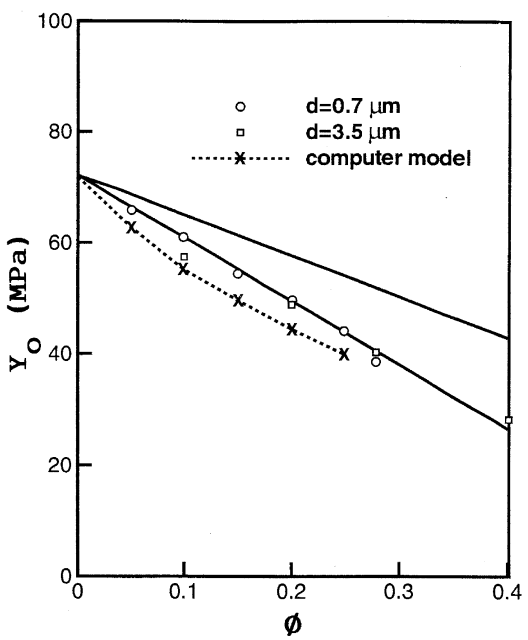

Fig. 7. Systematic decrease in yield stress for two PA-6 blends modified with stiff $CaCO_3$ particles of 0.7 and 3.5 μm size as a function of particle volume fraction ϕ [63], compared with result of a FEM model [74] (from Wilbrink et al. [63], courtesy of Elsevier).

if the reversal is carried out before yielding, it became clear that the particles were not adhered to the Nylon matrix but were being held in place by a clamping thermal misfit pressure exerted by the matrix on the particle. This clamping pressure p can be readily determined to be:

$$p = \frac{(\gamma_p - \gamma_c)\Delta T K_p}{\left(1 + \frac{4\mu_c}{3K_p}\right)} \tag{8}$$

and accounted well for the apparent tensile debonding stress σ_{db} of

$$\sigma_{db} = 3p\left[1 + \frac{2(1 - 4\nu + \nu^2)\left(\frac{K_p}{K_c} - 1\right)}{(1+\nu)\left[2(1-2\nu) + (1-\nu)\left(\frac{K_p}{K_c}\right)\right]}\right]^{-1} \tag{9}$$

where γ_p and γ_c are the volumetric coefficients of thermal expansion of the particle and polymer matrix while K_p and K_c are the bulk moduli of the particle and the matrix and μ_c and ν are the shear modulus and Poisson's ratio of the matrix, respectively [63]. Very similar results were obtained also with iPP for the same levels of $CaCO_3$ particles, although in this case the evidence suggested actual adhesion of particles to the matrix and debonding at stress levels well under the yield stress [66a,b].

8.4. Specific work of fracture by plastic ligament stretch

A definitive way of determining the improvements in fracture toughness of particle-modified polymers is through the measurement of the J integral work of fracture by means of a plane strain or plane stress double-cantilever-beam (DCB) specimen shown in Fig. 8, having dimensions in the plane stress range as shown. Fig. 9 shows three

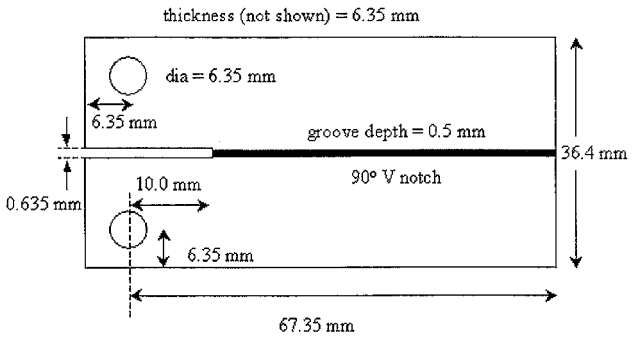

Fig. 8. Double-cantilever-beam (DCB) specimen used in determination of specific fracture work J of iPP blends (from Thio et al. [66a,b], courtesy of Elsevier).

load–displacement curves obtained from a variant of the specimen of the type of Fig. 8 for unmodified Nylon-6 and two blends containing 0.05 and 0.1 volume fractions of 0.7 μm $CaCO_3$ particles. Since the results with iPP and Nylon were very similar (apart from their plastic resistances at room temperature) we present rescaled results for either one or the other showing the most representative characteristics best. The unmodified Nylon curve shows a rather brittle fracture behavior in an unstable manner while the two modified blends show a clearly quite tough behavior with the blend with 0.05 particle concentration being the tougher. The load–displacement curves with the decreasing load-tail are clear signatures of tough behavior. The evaluation of the specific work of fracture, J, is obtained from the following relationship [31,32]

$$J = \alpha\varepsilon_0 Y_0(1-\phi)ch_1(a/b,n)(P/P_0)^{n+1} \tag{10}$$

with

$$P_0 = 1.072(\sqrt{1+a/c} - a/c)ct_s Y_0(1-\phi). \tag{11}$$

In Eqs. (16) and (17) α, ε_0, Y_0 and n, are material constants with ε_0 being the yield strain, Y_0, the yield stress, n, the strain hardening exponent, ϕ, the particle volume fraction, a, the effective crack length as shown in Fig. 8, b, the width of the specimen, $c = b - a$, h_1, a tabulated function of n and a/b obtained from numerical solutions of the crack tip problem [31,32] t, the specimen thickness, P, the peak load and P_0, the plane stress plastic limit load. Fig. 10 shows the results for iPP for the following values of $\alpha\varepsilon_0 = 0.011$, $Y_0 = 16.0$ MPa,[1] $n = 2.16$ for the material deformation responses and $a = 10$ mm, $b = 67.4$ mm, $t_s = 5.35$ mm (across the bottoms of the side grooves) and $h_1 = 1.83$ obtained by interpolation for the geometrical specimen parameters [31,32]. The figure shows a very substantial rise in J between the unmodified iPP and the first set of blends of modified polymer with $\phi = 0.05$ particle concentrations. Examination of the fracture surfaces of the unmodified samples showed a smooth surface containing only a set of shallow striations for the unmodified PA-6 while the fracture surfaces of samples containing particles with volume fraction ranging from 0.05 upward to 0.3 showed extensive ligament stretching between the cavities left behind by the debonded particles. Fig. 11(a)–(c) shows the SEM fracture surfaces of the corresponding PA-6 blends modified with the 0.7 μm $CaCO_3$ particles (determined from experiments with single edge notched tensile samples). Fig. 11(a) shows a reference cryogenically fractured surface of PA-6 of very smooth and brittle character while Fig. 11(b) and (c) shows the fracture surfaces of blends with 0.05 and 0.15 particle volume fraction. The dramatic stretches of the ligaments are striking in the cellular morphology.

The initial phases of plastic cavity expansion in the cellular material resulting from particle debonding in PA-6 have been modeled by Tzika et al. [75] for fully developed plastic behavior by means of a finite element approach taking proper account of the expected plastic anisotropy in the debonded particle environments. For our purpose to develop some understanding of the toughness behavior resulting from the large ligament stretches up to fracture we use a simple idealized 2D model shown in Fig. 12. Here the particles in the blend are idealized as a set of parallel rigid cylindrical rods of diameter d in a hexagonal packing with nearest interparticle ligament distance Λ in the initial condition. We take this as a good approximation to the regularly porous solid resulting from particle debonding as it begins to plastically stretch. We take the crosshatched hour-glass shaped region as a representative matrix ligament that is a candidate for extensive plastic stretching.

In this representation the volume fraction ϕ of particles becomes the initial level of porosity of the cellular solid given as [63]

$$\phi = \frac{\pi}{2\sqrt{3}} \frac{1}{\left(1+\dfrac{\Lambda}{d}\right)^2} \tag{12}$$

while the volume V of the representative 2D ligament becomes

$$V = \frac{\pi d^2}{4}\frac{(1-\phi)}{\phi} \tag{13}$$

Using a simple orientation hardening model for the stretching ligament discussed elsewhere [68], we find the plastic work of fracture W_p of the ligament, stretched to fracture at the locking stretch of λ_n to be

$$W_p = \frac{\pi d^2 Y_0}{4}\frac{(1-\phi)}{\phi}\ln(\lambda_n) \tag{14}$$

finally, the essential work of fracture J_e at the fracture plane is attained as

$$J_e = \left(\frac{\sqrt{3}\pi}{8}\right)^{1/2}\frac{(1-\phi)}{\sqrt{\phi}} Y_0 d\ln(\lambda_n) \tag{15}$$

Moreover, consideration of the additional plastic defor-

[1] This value was chosen as a best fit to the parabolic hardening model regime for the J integral evaluation. The actual yield strength is considerably higher as shown in Table 1.

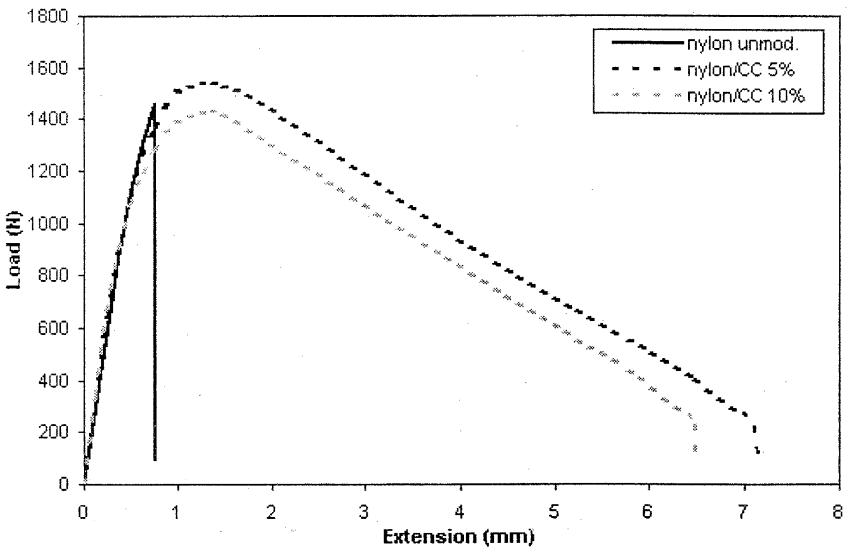

Fig. 9. Load–extension curves of single-edge-notched-plate (SEP); unmodified curve shows no sign of toughness while particle modified curves with volume fractions 0.05 and 0.10 show very gradual load drops with increasing extension, indication of tough behavior (from Wilbrink et al. [63], courtesy of Elsevier).

mation work in the deformed flanks outside the immediately rupturing layer of thickness $2\delta = (\sqrt{3}d/2)\sqrt{\pi/2\sqrt{3}\phi}$ gives the overall specific fracture work J as

$$J = J_e(1 + 2\ln(\varepsilon_f/\varepsilon_0)) \tag{16}$$

where $\varepsilon_f = \ln(\lambda_n)$ is the (ultimate plastic strain of failure of the ligament with ε_0 being the elastic strain at yield [63].

Considering as a check the blends with a volume fraction of $\phi = 0.05$ we use for the material parameters of $\varepsilon_0 = Y_0/E = 0.011$ for $E = 1437$, $Y_0 = 16$ MPa and $d = 0.7$ μm together with $\lambda_n \approx 7$ as estimated from the SEM micrographs of the ruptured ligaments we obtain by using Eq. (16) $J = 867$ J/m^2 which checks remarkably well with the value shown in Fig. 10. The J values for other blends can then be

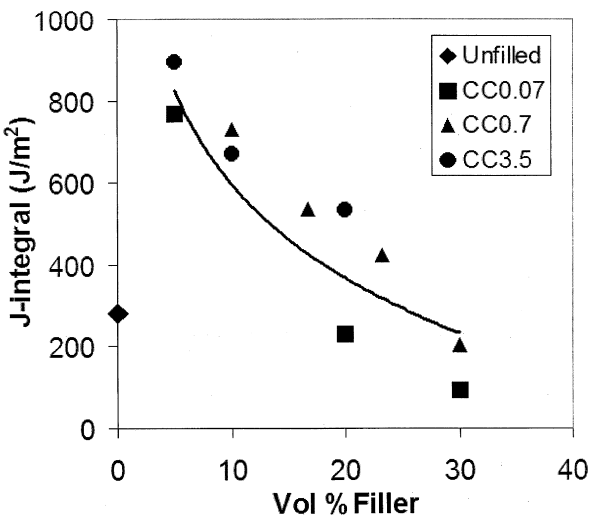

Fig. 10. The dependence of the specific work of fracture J for iPP blends as a function of particle volume fraction for three different particle diameters, in microns. The solid curve represents the prediction of Eqs. (14) and (15) (from Thio et al. [66a,b], courtesy of Elsevier).

determined as scaled down versions of this figure based on their (volume) fractions. The obtained trend is shown in the figure with the solid curve. While the calculated dependence falls somewhat under the actual values it gives broadly the same trend. Clearly, with increasing volume fraction the toughness decreases systematically since the increasing particle concentration, converting directly into porosity, decreases the volume fraction of the energy absorbing plastically stretching polymer component, a trend well known in the ductile fracture of metallic alloys [76]. Extrapolating the expression in Eq. (16) to smaller volume fractions gives unbounded results, also a well known fact indicating that the negative pressure required to expand a porous solid plastically diverges as ϕ goes to zero. Thus, the toughness J of the unmodified polymer is not a 'member' of the family of results for the pre-cavitated particle-modified polymers. The neat polymer undergoes brittle behavior. Clearly, at a certain critical volume fraction $0 < \phi_c < 0.05$ a sharp bifurcation in behavior should occur that transforms the response from a brittle-like crack propagation into the plastic ligament stretching response of a cellular material.

8.5. The critical particle volume fraction ϕ_c

We note first that while the unmodified polymer exhibits brittle-like behavior it actually undergoes considerable plastic accommodation at the crack tip within a zone r_p of some extent at the instance of fracture instability. Thus, examining the brittle and tough behavior in the same framework of the Hutchinson–Rice–Rosengren (HRR) [77,78] developments, the extent of the plastic zone r_p is determined first by equating the effective stress σ_e (deviatoric tensile stress) at the crack tip to the yield

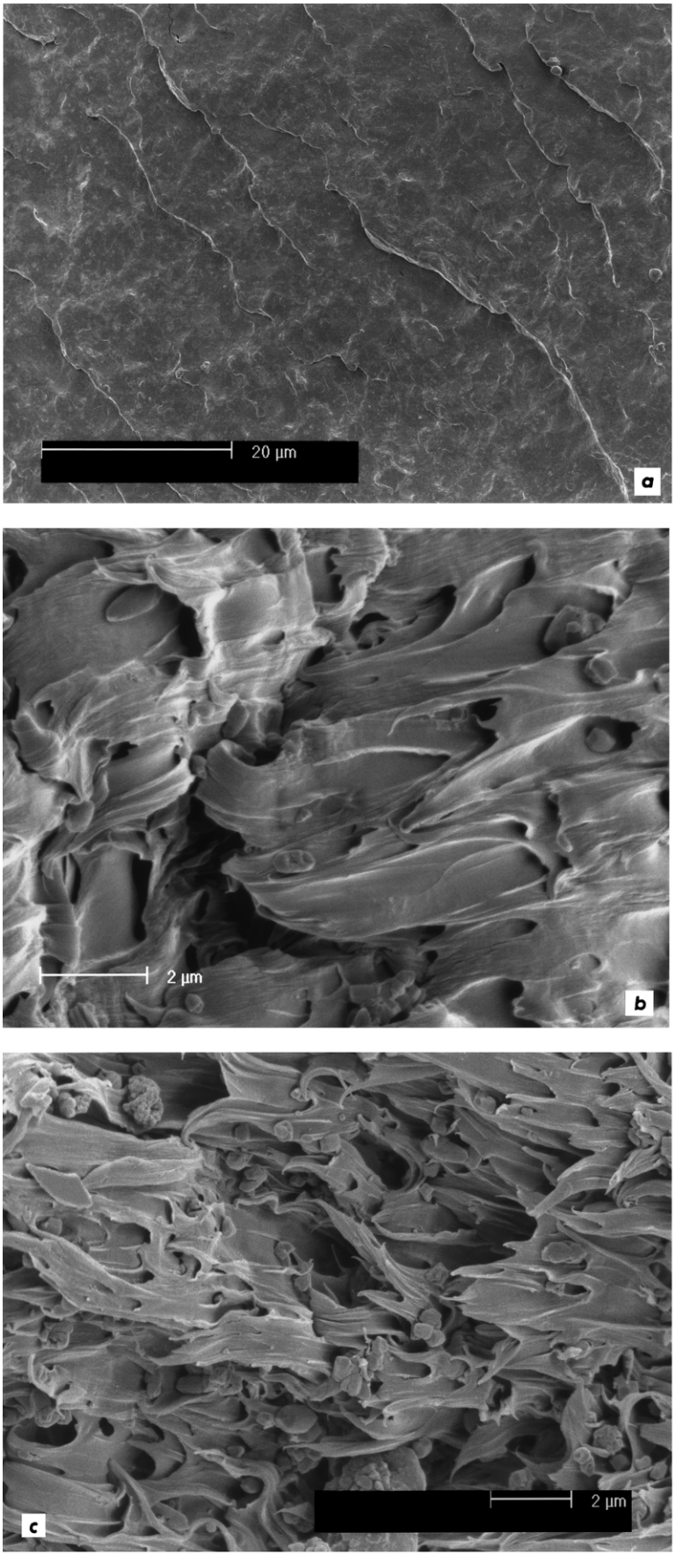
20 μm
a
2 μm
b
2 μm
c

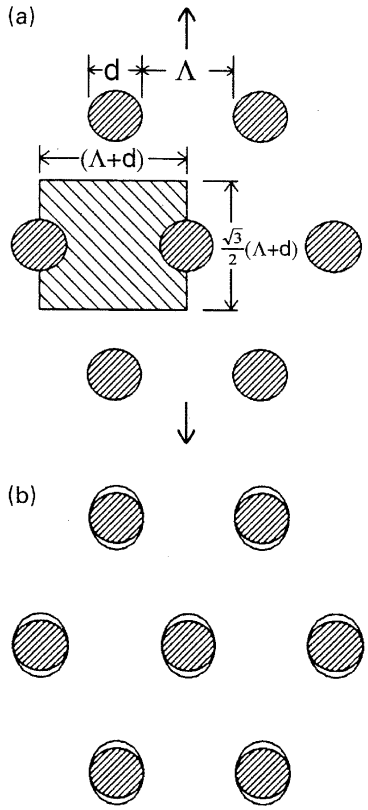

Fig. 12. A 2D model of the distributions of stiff particles in the plastically deformable matrixes of PA-6 or iPP: (a) before deformation showing shaded the representation ligament volume and defining the inter-particle ligament thickness Λ; (b) early stretching after debonding of particles at the inception of ligament stretching (from Wilbrink et al. [63], courtesy of Elsevier).

strength Y_0 and solve for r_p [77]

$$\sigma_e = Y_0\left(\frac{J}{\varepsilon_0 Y_0 I_n r_p}\right)^{1/n+1} \tilde{\sigma}_e(\theta, n) \tag{17}$$

where $I_n = \pi(n+1)/n$ is an integral that serves to normalize the peak value of the distribution of the effective stress σ_e around the crack tip to unity, and $\tilde{\sigma}_e(\theta, n)(= 1.0)$ represents that maximum value in the distribution at an angle $\theta = \pi/2$ as shown in Fig. 13 [32]. For the specific material parameters of interest here we consider those given already above, i.e. $J = 300\ \mathrm{J/m^2}$, the work of fracture of the unmodified material, gives $r_p = 370\ \mu\mathrm{m}$.

We then identify the 'brittle' response within this plastic zone as a local cavitation event when the mean normal stress (the negative pressure) σ_m reaches the cavitation strength $\hat{\sigma} = \beta K_0$ (= 94.4 MPa) [25] at the extension of the crack at $\theta = 0$. We determine the critical distance r_c in front of the crack tip in the plastic zone where this condition is reached from the corresponding expression to Eq. (17) for the

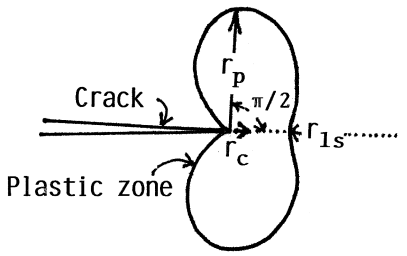

Fig. 13. Sketch of a plastic zone around a tensile crack showing the location and meaning of r_c and r_p.

distribution of the mean normal stress in the plastic domain

$$\sigma_m = Y_0\left(\frac{r_p}{r_c}\right)^{1/n+1} \tilde{\sigma}_m(\theta = 0, n) \tag{18}$$

where we replaced $J/\varepsilon_0 Y_0 I_n$ with r_p, as determined above, and note that $\tilde{\sigma}_m(\theta = 0, n) = (\tilde{\sigma}_{rr} + \tilde{\sigma}_{\theta\theta})/2 = 1.75$ [32], we obtain then $r_c = 8\ \mu\mathrm{m}$. While this distance is somewhat large in comparison with structural inhomogeneities it is acceptable.

Now, to examine the competing conditions for the bifurcation phenomenon at a critical particle volume fraction, ϕ_c we state the criterion for the ductile ligament stretching as the reaching of effective stress $\sigma_e = Y_0$ at $\theta = 0$ at the crack tip over a distance $r_{ls} = \Lambda + d$, the projected dimension across the fracture plane of the representative volume of the stretching ligament, i.e.

$$\sigma_e = Y_0 = Y_0\left(\frac{J_d}{\varepsilon_0 Y_0 I_n r_{ls}}\right)^{1/n+1} \tilde{\sigma}_e(\theta = 0, n) \tag{19}$$

where $r_{ls} = \Lambda + d = d(\pi/2\phi\sqrt{3})^{1/2}$ and $\tilde{\sigma}_e(\theta = 0, n) = 0.25$ [32] and where, of course, $n = 2.16$ as presented already above. Solving for the J_d for plastic ligament stretching response to commence we have

$$J_d = \varepsilon_0 Y_0 I_n d(\pi/2\sqrt{3}\phi)^{1/2}[\tilde{\sigma}_e(\theta = 0, n)]^{-(n+1)} \tag{20}$$

The bifurcation between brittle-like response and the ligament stretching ductile response should occur at a critical volume fraction ϕ_c where $J_d = J_b = 300\ \mathrm{J/m^2}$ where the condition for initiating the ductile ligament stretching response is just met simultaneously with the brittle response and *initiates* a toughness jump to the full value of J given by Eq. (16). The critical particle volume fraction that will achieve this is $\phi_c = 0.017$ for the material parameters listed above, characteristic of iPP. While the accuracy of this estimate is not considered to be high, it is eminently in the correct range. It is fair to point out here that the analyses above utilized values of Y_0, n, etc. consistent with the parabolic phenomenological fit discussed in Ref. [66a,b]. These values differ from those given in Table 1 for

Fig. 11. SEM fractographs of PA-6 blends: (a) a cryo-fracture surface of an unmodified sample showing a purely brittle appearance; (b) fracture surface of blend with 0.05 volume fraction of particles with 0.7 μm diameter stressed in tension at room temperature; (c) fracture surface of a blend modified with 0.15 volume fraction of particles, both showing extensive and dramatic ligament stretching (from Wilbrink et al. [63], courtesy of Elsevier).

which a phenomenological parabolic fit to the stress–strain curves would be different.

8.6. The Izod impact toughness

While the nature of it leaves much to be desired from a quantitative mechanistic point-of-view—the Izod impact experiment is widely used to evaluate the toughness of blends. The principal goal of the experiment is to produce a standard extreme condition to probe the degree of success of the toughening modification. While the experiment has many imperfections such as resulting often in no separation but mere plastic hinging at the notch for tough responses, the conditions of the test approximate to those of a crack subjected to a high strain rate at its tip, the notch root. When local micro-crack-like imperfections exist at the notch root the approximation becomes better.

Here our interest is primarily in the response of rigid particle-modified blends of some semi-crystalline polymers with well known brittleness problems where the modifying particles are $CaCO_3$, and tend to create more demanding conditions.

In experiments with $CaCO_3$ particle-modified HDPE Bartczak et al. [68,69] have demonstrated a very successful toughening behavior exhibiting dramatic toughness jumps in connection with the critical ligament size criterion of Wu [56,57] for both rubber particles and rigid particles with almost identical level of success. In contrast with this successful example Muratoglu et al. [58,59] obtained successful toughening behavior of PA-6 only with rubbery particles in Izod toughness experiments. In a complementary set of experiments with PA-6 Wilbrink et al. [63] using $CaCO_3$ particles observed dramatic ligament stretching behavior in the usual quasi-static tension experiments and in J-integral toughness measurements with DCB samples. However, their results with Izod impact experiments were very disappointing[2] showing only very limited improvements of Izod toughness with stiff-particle-modification that could be accounted for entirely by crack tip shielding alone. Characteristically, brittle-appearing fracture surfaces showing extensive particle debonding but no plastic ligament stretching was observed. A very similar but even a bit more disappointing behavior was encountered by Thio et al. [66a,b] in Izod impact experiments on $CaCO_3$ particle-modified iPP.[3] Here too, while quasi-static J-integral experiments with DCB samples have demonstrated dramatic toughness increases with particle modification above volume fractions of $\phi > 0,05$ as already remarked above (Fig. 10). The Izod impact experiments showed only modest toughening[3] with 0.7 μm diameter $CaCO_3$ particles without any observable ligament stretching behavior on the fracture surfaces—even though considerable particle debonding was again evident. While this general behavior of toughening response ranging from very successful for HDPE to disappointing response with iPP and very disappointing response with PA-6 fits a general trend consistent with the inelastic response of the respective polymers as we will discuss below, a common aggravating feature was the severe embrittling effect of clustering of the rigid particles into quite large unbonded inclusions. These, upon separating from the matrix often acted as supercritical particles intiating brittle response, even in quasi-static tension experiments as discussed by Wilbrink et al. [63]. Often such large particle clusters were found at notch roots in the Izod samples where they further aggravated an already brittle response, an example of which in PA-6 is shown in Fig. 14 [63].

[2] 100–120 J/m for a particle volume fraction of 0.2 rather than ca. 800 J/m for the same volume fraction of stiff-particle-modified HDPE of Bartczak et al. [69].

[3] ca. 75 J/m for a 0.25 volume fraction of the same type of stiff particles used by Wilbrink et al. [63].

9. Discussion

9.1. Conditions of the Izod impact experiment

That the Izod impact experiment accentuates the conditions for brittle response is well appreciated but there are few satisfactory treatments of the quantitative nature of the effect, particularly when plastic flow occurs at the notch root. For large local geometrical changes in the specimen shape due to extensive plastic deformation the analysis of the problem requires special numerical techniques different for different polymers. Here we consider a useful development that should be applicable short of full plastic hinging at the notch.

Considering the Izod bar as a rigidly clamped cantilever beam with a notch of depth a at the plane of clamping, of free length L, depth h and thickness b with the impacting force F considered applied at the end of the bar, a distance L away from the clamping plane, the terminal flexure δ under the force F is by elastic cantilever beam relations given by

$$\delta = \beta(a/h)\frac{FL^3}{3EI} \tag{21}$$

where E is the Young's modulus and I, the bending moment of inertia. The factor $\beta(a/h)(= 1.233)$ [29] accounts for the additional flexure due to a notch of depth a in a beam of depth h. Removing the elastic consideration by normalizing with the outer element beam bending stress, a geometrical expression for nominal bending strain is obtained at the clamping plane

$$\varepsilon = \frac{3}{2}\frac{h}{L^2}\frac{\delta}{\beta(a/h)} \tag{22}$$

With the notch depth a and the notch radius ρ present, the concentrated strain at the notch root, for elastic

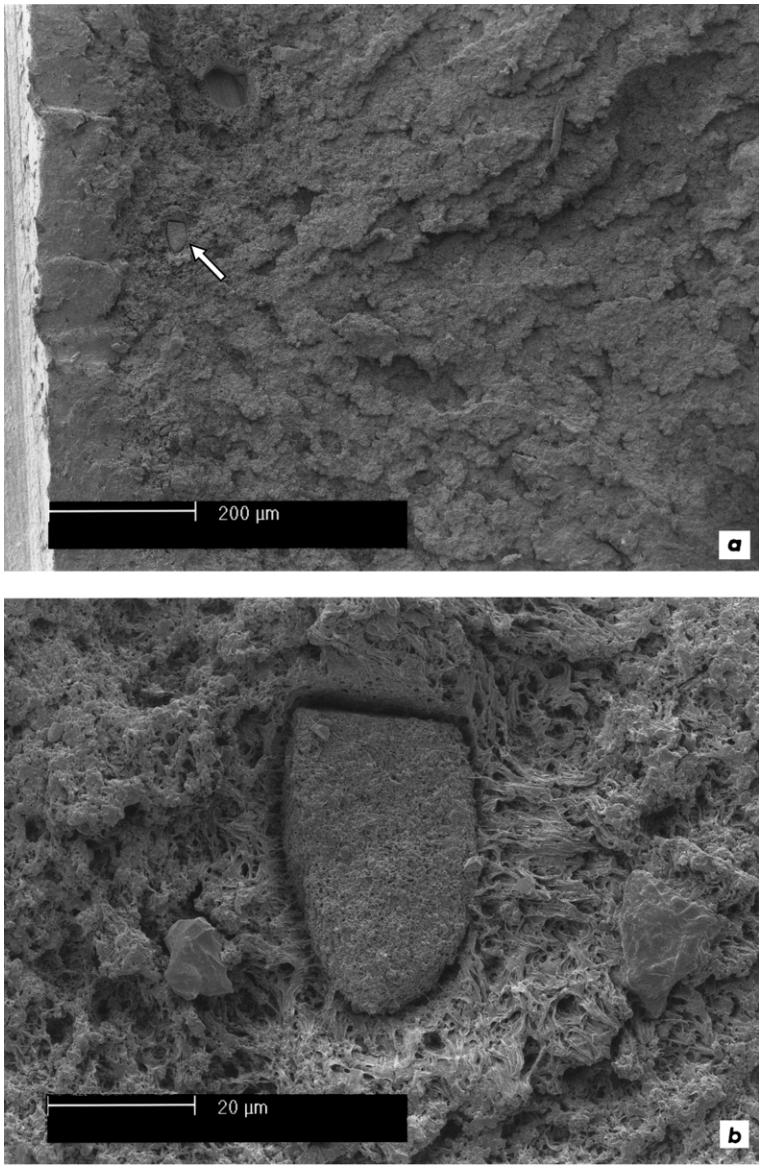

Fig. 14. SEM fractographs of the region near the notch of an Izod impact specimen of PA-6: (a) area near the notch where a large cluster of small particles has triggered brittle propagation; (b) the same large particle enlarged, showing that it is a cluster of the small stiff modifying particles of the blend.

considerations should be [27]

$$\varepsilon = \frac{3}{2}\frac{h}{L^2}\frac{\delta}{\beta(a/h)}(1+2\sqrt{(a/\rho)}) \tag{23}$$

However, if there is local plasticity, and the expression is considered as a rate expression the local notch root strain rate $\dot{\varepsilon}_I$ should be for the Izod bar

$$\dot{\varepsilon}_I \cong \frac{3}{2}\frac{h}{L^2}\frac{v}{\beta(a/h)}(1+2(a/\rho)^{(m/m+1)}) \tag{24}$$

where we have used the developments for cracked, rate dependent solids [32] where $m(=\mathrm{d}\ln\dot{\varepsilon}/\mathrm{d}\ln\sigma)$ is the stress exponent of the strain rate expression of plastic flow and v, the striker velocity at the end of the bar—typically 3.5 m/s. As we see in Table 2 the local strain rate amplification at the notch, in comparison with a typical strain rate of 10^{-3} s^{-1} in a tension experiment is around 2×10^6, or quite substantial.

9.2. Brittle or tough Izod response of semi-crystalline polymers

As an illustration of a more quantitative approach to the potentials for toughening of brittle polymers, we examine here six semi-crystalline polymers the phenomenological plastic response of which have been reported by G'Sell and Jonas [79]. All of these polymers are known to be brittle at low temperature and are notch brittle in impact in neat form. Their yield stresses Y_0 strain rate sensitivities of the yield stress (or flow stress) $\mathrm{d}\sigma/\mathrm{d}\ln\dot{\varepsilon}$ the phenomenological stress exponents $m = \mathrm{d}\ln\dot{\varepsilon}/\mathrm{d}\ln\sigma$ of the strain rate during plastic

Table 2
Izod impact fracture parameters for neat semi-crystalline polymers of Table 1

Polymer	$(1+2(a/\rho)^{m/(m+1)})$	$(\dot{\varepsilon}_I)/(\dot{\varepsilon}_0)^a$	Y_0 (MPa)	$Y_I{}^b$ (MPa)	ΔY (MPa)	$Y_I+\Delta Y$ (MPa)	$\hat{\sigma}=\beta K_B$	ε_{f0}	ε_f
PA-66 (Nylon- 66)	20.3	2.35×10^6	103	171	22.7	193.7	182	0.82	~0
PA-6 (Nylon-6)	19.7	2.29×10^6	73.0	121	32.0	153.0	181	1.16	0.563
PVC	20.0	2.32×10^6	57.1	95.9	18.2	114.2	145	0.94	0.515
HDPE	19.5	2.13×10^6	30.8	74.7	28.8	103.5	127	1.85	1.14
PP	18.4	2.26×10^6	38.3	85.6	19.3	105.0	122	1.50	0.765
LDPE	17.9	2.08×10^6	11.9	59.5	13.7	73.2	92.7	1.80	1.205

[a] $\dot{\varepsilon}_0=10^{-3}\ s^{-1}$.
[b] As explained in text.

flow and their initial strain hardening rates $d\sigma/d\varepsilon$ as derived from G'Sell and Jonas, are given in Table 1 for experiments conducted at room temperature (295 K) [79]. The table also lists the activation volumes $\Delta\nu^*(=KTd\ln\dot{\varepsilon}/d\sigma)$ at yield and the bulk moduli K_B [80] for reference. These activation volumes must be considered as special values at room temperature when consideration is given to a more complete analysis [18]. For the phenomenological strain hardening behavior, giving the shapes of true-stress, true-strain curves of these polymers G'Sell and Jonas have found a convenient functional form given as

$$\sigma = Y_0(\dot{\varepsilon},T) + K(\exp 2\varepsilon - \exp(-\varepsilon)) \tag{25}$$

with the values for K being given in the last column of Table 1, where ε is considered as the total true plastic strain and the small strain elastic behavior is ignored. The form of Eq. (25) implies (incorrectly) that the entire temperature and rate dependence of the plastic resistance resides in a rate dependent component of the resistance manifested by the yield stress Y_0 and that the hardening component, attributable to an internal stress type formalization, widely used in metal plasticity is temperature independent. While this is strictly not correct [18] it is a convenient abstraction for our purposes.

The best and most quantitative test for the level of toughening achievable by particle modification is the quasi-static J integral experiment discussed in Section 8.4 where a transition between the unmodified blend and the particle modified blends is quite clear, as shown in Fig. 10 for the iPP blends. The question is whether or not that same beneficial response can also be present under the more extreme condition at the notch of an Izod experiment, and, if not, for what reason? The question must be answered at the level of the stretching ligaments. For this we recognize first that even under ideal behavior each of the six polymers of Table 1 has a terminal fracture strength. While this strength will be strictly governed by chain scission in the stretched ligaments at a stress level in considerable excess of the cavitation strength of the unoriented polymer given by Eq. (3b), this information is not readily available. Therefore, (a bit arbitrarily) we take for the fracture strength of the stretched ligament the same tensile cavitation stress, and in a further level of approximation take for this the negative pressure $\hat{\sigma}$ required to initiate cavitation. We note that while this choice appears arbitrary, it is operationally quite sensible, since at the final levels of stretch of the ligaments the local 'modulus' is so high that the actual level of fracture stress chosen does not influence much the final plastic strain to fracture, and thus, the plastic work of ligament rupture. For this procedure, as we discussed in Section 4, we take the computer simulation as a guide for the cavitation behavior of amorphous PP as:

$$\hat{\sigma} = \beta K_B \tag{26}$$

where $\beta=0.028$ was found to be the appropriate coefficient determined in the simulation [23]. Assuming that this factor will be the same for all other semi-crystalline polymers and applicable to their amorphous components, based on the published experimental determinations of the bulk moduli K_B, gives the tensile cavitation strength estimates for six materials listed in column 8 of Table 2.

The ideal plastic rupture of a stretched matrix ligament is sketched in Fig. 15 at a given temperature ($T=295$ K for the cases presented in Table 1). The ligament yields at Y_0 in tension at a strain rate of $\dot{\varepsilon}_0=10^{-3}\ s^{-1}$ and plastically stretches, advancing along the true-stress, true-strain curve along a characteristic hardening contour until the cavitation strength $\hat{\sigma}$ is reached. The associated strain to fracture is obtained from Eq. (25) by equating the stress to the

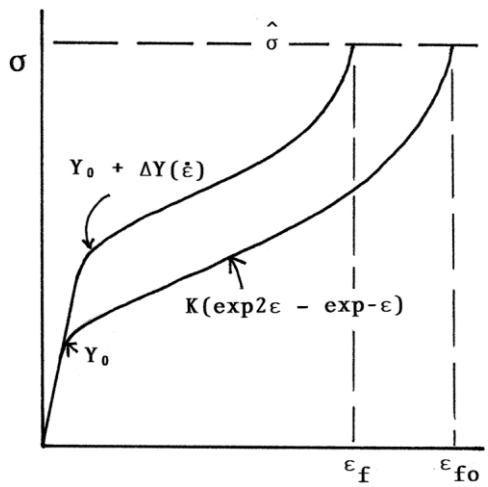

Fig. 15. Sketch of ideal stress–strain curve of a stretching ligament.

cavitation strength of Eq. (26). These calculated levels of strain to fracture of a stretched ligament under the tensile strain rate of $\dot{\varepsilon}_0 = 10^{-3}\ s^{-1}$ are shown in column 9 of Table 2. In every case even for PA-66 these strain levels are substantial. On the other hand in the Izod impact experiment at the enhanced local notch tip strain rate $\dot{\varepsilon}_I$ the plastic resistance will be substantially increased by a combination of two separate but related effects. First, purely by dynamic mechanical effects the material shear modulus will increase from its usual level of μ_0 shown in column 2 of Table 1 to a level μ_I given in column 3 of Table 1, obtained by a modulus shift from the usual 1 c/s modulus to the 2×10^3 c/s modulus, of the natural frequency of a typical polymer Izod bar considered as an oscillating cantilever beam (see Appendix A). These changes in shear moduli, determined for each polymer individually based on the available dynamic modulus spectra [85], are substantial. Furthermore, the increased shear moduli will proportionally raise the yield stresses from Y_0 to Y_I given in Table 2 on the known linear dependence of the plastic resistance on the shear modulus. Second, the plastic resistance will increase at the notch tip due to the strain rate dependence of the flow stress resulting from the thermally activated nature of the plastic strain rate through the strain rate dependence of the plastic resistance, given for each polymer in column 10 of Table 1. The resulting elevation of the plastic resistance ΔY for each polymer due to the strain rate sensitivity alone is given in column 6 of Table 2 resulting in the total elevation of the plastic resistance at the notch root, to $Y_I + \Delta Y$, given in column 7 of Table 2 for each polymer. As the ligament stretches under these conditions it undergoes additional strain hardening that can be evaluated according to the phenomenological expression of G'Sell and Jonas of Eq. (25) until the appropriate fracture stress $\hat{\sigma}$ is reached at a tensile strain of ε_f. This final fracture strain is shown in column 10 of Table 2. In every case the reduction of strain to fracture from the tension experiment to the Izod case, apparent from comparison of columns 9 and 10 of Table 2 is quite substantial. In the case of PA-66 the estimate for ε_f is zero indicating purely brittle response. The reductions for PA-6, PVC and PP are all significant but still remain reasonably attractive. However, there are additional subsidiary conditions that result in further embrittlement when rigid particles are used. We discuss these in Section 9.3 below.

9.3. Bifurcation of response between brittle or tough behavior at the Izod notch root

To provide a rationale for further embrittlement we need to adopt a consideration similar to what was used in Section 8.5 in the determination of the critical particle volume fraction for tough behavior, and also take note of the fact that the polymers under consideration are all intrinsically brittle and will undergo ductile to brittle transitions under certain perturbations similar to what is encountered in steels [81].

Thus, consider the notch tip conditions to be similar to the crack tip shown in Fig. 13. Under ideal conditions, as discussed in Section 9.2 above, the root of the Izod notch with a smooth surface should undergo large strain plastic flow even at the local enhanced plastic resistances, as long as the flow stress remains under the cavitation level in the stretching ligaments between separated particles of a heterogeneous blend.

However, consider now the various perturbations that can arise due to the particles and their clusters. For example, if along the notch surface a significant concentration of particle clusters with weak interfaces had disrupted the smooth surface, the notch can already act as a sharp crack equal to the notch depth and initiate brittle propagation. A more serious perturbation, however, will be the effect of large particle clusters with weak interfaces that can trigger a transition from ductile tearing of ligaments to brittle behavior if it exceeds in size a critical value given by:

$$d = \frac{2}{\pi} \frac{JE}{(1 - \nu^2)Y^2} \tag{27}$$

where J is the critical work of fracture of the neat polymer, E, the elastic modulus of the blend and Y, the enhanced prevailing plastic resistance somewhere between the level Y_I and $Y_I + \Delta Y$ given in Table 2. Taking for PA-6 and iPP blends the following values of: $J = 34.8\ J/m^2$, $E = 1.68$ GPa, $Y_I = 121–153$ MPa [63]; and $J = 300\ J/m^2$, $E = 1.48$ GPa, $Y_I = 85.6–105$ MPa, respectively, we calculate the critical particle clusters to be in the size ranges of 2–4 μm for PA-6 and 28–40 μm for iPP, depending on the actual level of the prevailing enhanced plastic resistance. Particle clusters in these size ranges were widely encountered, even up to 100 μm in size [66a,b]. Thus, it becomes clear why the Izod impact toughnesses of these blends were generally very low and the fracture surfaces had an apparent spongy and brittle appearance, even though in slow tension or in quasi-static J integral fracture toughness experiments attractive toughness was observed. This triggering of a transition from ductile tearing behavior to sudden brittle fracture is very familiar in structural steels in the strain fields of blunted notches undergoing tough behavior [81]. Ideally in blends with very uniform dispersions of particles such occurrences should be rare. These beneficial conditions, however, are only attainable with cavitating rubbery particles that can indeed be uniformly dispersed in conventional processing practice.

Another complication of an embrittling nature with rigid particle modification results to some degree in the initial phases of incipient tough behavior by partial particle debonding discussed by Wilbrink et al. [63]. This occurs when the partly debonded particles prevent lateral plastic contraction of the cavities. This lateral plastic pinching of the particles by the surrounding matrix in turn sets up a compensating level of negative pressure in the cellular matrix that elevates further the axial plastic resistance in the

principal strain direction. This effect of additive mean normal stress σ_m which should last only for the duration of transition to the general plastic flow is difficult to evaluate accurately, but could be as large as [63]

$$\sigma_m = 0.8\alpha\beta Y\sqrt{\phi} \tag{28}$$

where the α and β coefficients could be in the range of 0.3 and 2.5 and the plastic resistance Y as high as the impact enhanced levels given in Table 2. These α and β coefficients are unrelated to those discussed in Section 4. Again, this adverse factor would not be present in rubber particle modified blends, where lateral cavity contraction would be unhindered.

9.4. The critical interparticle ligament dimension criterion for toughening

In the critical interparticle ligament dimension criterion discovered by Wu [56,57] a dramatic impact toughness jump results in a blend when the interparticle ligament dimension becomes less than a critical value, regardless of particle size and particle volume fraction. Clear demonstrations of this were verified for rubbery particles by Muratoglu et al. [58,59] in PA-66 blends and by Bartczak et al. [68,69] in HDPE blends with both rubbery and rigid particles. The source of this phenomenon was identified conclusively by these latter investigations to lie in a preferentially crystallized layer around the particles with advantageously low plastic resistances that were considered to be responsible for the effect. While no specific searches were made for such an effect in rigid particle-modified blends of PA-6 and iPP [63,66a,b] there was no supporting evidence for it since in these blends the Izod impact toughnesses were uniformly disappointing and all other correlations left no room for the special effect. It is likely that with the severe embrittling effects of particle clusters and the attendant increases in interparticle distances to always lie above the critical level, this criterion could apparently not be satisfied and the phenomenon was absent.

Finally we note a compensating advantageous effect aiding the toughness behavior in the Izod experiment. Examination of the shapes of the stretched ligaments in PA-6 in Fig. 11(b) and (c) suggests a taffy-like stretch of the ligaments, indicating that if a successful ligament stretching can be initiated it might get the benefit of softening by adiabatic heating.

10. Conclusions

For fundamental reasons of bonding, unoriented polymers are intrinsically brittle solids that will always exhibit a ductile to brittle transition.

As with all intrinsically brittle solids since the brittle strength has little temperature and strain rate dependence and is difficult to increase through changes in chemistry or microstructure perfection, the most effective avenue to suppress a ductile to brittle transition is to lower the plastic resistance.

While there are several possibilities of lowering plastic resistance through diluent induced forms of plasticization these have limited ranges of applicability [48–50,52], the generally most effective way to reduce the plastic resistance is through means of quasi-uniformly cavitating the solid by incorporation of equiaxed particles that can be made to cavitate or debond to convert the polymer into a cellular solid [58,59,63,66a,b,68,69,74,75]. In many instances, as in epoxies with high flow stresses and strain hardening rates, such cavitation alone can result in attractive levels of toughening by crack tip shielding [71]. In semi-crystalline polymers, however, dramatic effects can be achieved with either rubbery or rigid particles when the quasi-uniformly cavitated cellular polymer can undergo wide spread large strain plastic extension of interparticle ligaments in slow tension resulting in impressive crack extension resistances J [58,59,63,66a,b]. This phenomenology is quite similar to promotion of ductile fracture by plastic cavity growth following inclusion separation in metallic alloys [16].

There are important limitations on exploiting the toughening mechanisms by quasi-uniform cavitation and plastic ligament stretching under impact conditions with initially unoriented semi-crystalline polymers, which have well defined fracture ceilings of stretching ligaments governed by intrinsic molecular level cavitation. These limitations arise from the high notch-tip plastic strain rates which are in the range of $2-3\times10^3\ s^{-1}$ and in comparison with the usual tension experiment strain rates of ca $10^{-3}\ s^{-1}$ amount to a six orders of magnitude jump. Under these conditions, the shear moduli will increase typically by a factor of 2, or larger, and some polymers even undergo a reverse glass transition in their amorphous components. This and the separate effect of the plastic strain rate-dependence of the plastic resistance can elevate the effective plastic resistance close to the fracture ceiling. In PA-66 it is estimated that these effects reduce the local strain to fracture to zero.

In semi-crystalline polymers modified with cavitating rubbery particles such as PA-6, HDPE, PVC, PP attractive levels of tough response in Izod impact are still achievable with quasi-uniform dispersion of particles [58,62]. In polymers modified with debonding rigid particles, where clustering of particles into large super-critical size inclusions appears to be unavoidable, the perturbations due to clusters in nearly every case bridge the remaining difference between the strain rate-enhanced plastic resistance and the fracture ceiling by intrinsic cavitation and result in triggering of brittle behavior [63,66a,b] in a way very similar to triggering of brittle fracture in structural steels with fracturing large carbides or slag inclusions [81]. The unavoidability of large particle clustering is a basic imperfection due to flow channeling in the usual forms of

industrial polymer processing practices, making modification of blends with rubbery particles more attractive.

Acknowledgements

We acknowledge with thanks the many contributions of our collaborators: Drs Z. Bartczak, O.S. Gebizlioglu, L. Lin, O.K. Muratoglu, J. Qin, Mrs Y. Thio and M.L.K. Wilbrink, and our industrial associate M. Weinberg of DuPont. The researches that were responsible for these findings were supported by the NSF-MRSEC Program through the Center for Materials Science and Engineering at MIT from grant DMR-98-08942 and earlier versions.

Appendix A. Frequency dependent shear modulus shifts

The shear modulus shifts due to the high frequency response of the struck Izod bar had to be determined indirectly in each instance since for none of the polymers of interest were isothermal dynamic moduli spectra available as a function of frequency. The procedure adopted was to identify the principal molecular relaxation process of the glass transition in the amorphous components of each of the semi-crystalline polymers of interest. Determine the activation energy of that process and with it determine the characteristic temperature shift of the glass transition due to an increase in frequency from 1 to 2×10^3 c/s, characteristic of the oscillating Izod bar.

For PA-6 the transition of interest was the α transition with an activation energy of 45 kcal/mol, resulting in a temperature shift of $-29.6\,^{\circ}\mathrm{C}$ [82]. The temperature dependence of the shear modulus utilized to determine the increased stiffness was obtained from Ref. [18]. The same response was assumed for PA-66.

For HDPE and LDPE the transition of interest was the γ transition with an activation energy of 12 kcal/mol [82], giving a $\Delta T = -110\,^{\circ}\mathrm{C}$, with the modulus shifts determined from Ref. [82] or Ref. [85].

For PVC the transition of interest was the β transition with an activation energy of 15 kcal/mol [82], giving $\Delta T = -89^{\circ}\mathrm{C}$ with the modulus shift determined from Ref. [83].

For iPP the relaxation of interest was also the β transition with activation energy of 28 kcal/mol [82], giving $\Delta T = -47.6\,^{\circ}\mathrm{C}$ with the modulus shift determined from Ref. [85].

References

[1] Bucknall CB. Toughened plastics. London: Applied Science; 1977.
[2] Riew K, editor. Rubber toughened plastics. Advances in Chemistry Series 0065-2393, vol. 222. Washington, DC: ACS; 1989.
[3] Riew K, editor. Toughened plastics I: science and engineering. Advances in Chemistry Series 233, Washington, DC: ACS; 1993.
[4] Riew K, Kinloch AJ, editors. Toughened plastics II: novel approaches in science and engineering. Advances in Chemistry Series 252, Washington, DC: ACS; 1996.
[5] Pearson RA, Sue H-J, Yee AF, editors. Toughening of plastics: advances in modeling and experiments. ACS Symposium Series 75, Washington, DC: ACS; 2000.
[6] Argon AS. In: Mughrabi H, editor. Materials science and technology, vol. 6. Weinheim: VCH; 1993. p. 461.
[7] Perez J. Physics and mechanics of amorphous polymers. Rotterdam: A.A. Balkema; 1992.
[8] Mott PH, Argon AS, Suter UW. Phil Mag 1993;67:931.
[9] Hutnik M, Argon AS, Suter UW. Macromolecules 1993;26:1097.
[10] Argon AS. Phil Mag 1973;28:839.
[11] Argon AS, Bessonov MI. Phil Mag 1977;35:917.
[12] Boyce MC, Parks DM, Argon AS. Mech Mater 1988;7:15.
[13] Arruda EM, Boyce MC. In: LaMaitre J, editor. Handbook of materials behavior, nonlinear models and properties. New York: Academic Press; 2000. Section 5.9.
[14] Zhou QY, Argon AS, Cohen RE. Polymer 2000;42:613.
[15] Theodorou D, Suter UW. Macromolecules 1986;19:139.
[16] McClintock FA, Argon AS. Mechanical behavior of materials. Reading, MA: Addison Wesley; 1966.
[17] Bartczak Z, Argon AS, Cohen RE. Macromolecules 1992;25:5036.
[18] Lin L, Argon AS. Macromolecules 1994;27:6903.
[19] Ritchie SJK. J Mater Sci 2000;35:5829.
[20] Lee BJ, Argon AS, Parks DM, Ahzi S, Bartczak Z. Polymer 1993;34:3555.
[21] Ahzi S, Lee BJ, Asaro RJ. Mater Sci Engng 1994;A189:35.
[22] Bartczak Z, Cohen RE, Argon AS. Macromolecules 1992;25:4692.
[23] Galeski A, Bartczak Z, Argon AS, Cohen RE. Macromolecules 1992;25:5705.
[24] Ta J, Thio YS. Unpublished experiments.
[25] Mott PH, Argon AS, Suter UW. Phil Mag 1993;68:537.
[26] Rose JH, Smith JR, Guinea F, Feranti J. Phys Rev B 1984;28:29.
[27] Neuber H. Theory of notch stresses (English translation). Ann Arbor, MI: J.W. Edwards; 1946.
[28] Savin GN. Stress concentration around holes. London: Pergamon Press; 1961.
[29] Tada H, Paris P, Irwin G. The stress analysis of cracks handbook, 2nd ed. St. Louis, MO: Del Research Corp; 1985.
[30] Sih GC, Methods of analysis and solutions of crack problems, vol. 1. Leyden: Noordhoff; 1973.
[31] Kumar V, German MD, Shih CF. An engineering approach for elastic-plastic fracture analysis (NP-1931 research project 1237-1). Palo Alto, CA: Electric Power Research Institute; 1981.
[32] Riedel H. Fracture at high temperatures. Berlin: Springer; 1987.
[33] Kelly A, Tyson WR, Cottrell AH. Phil Mag 1967;15:567.
[34] Rice RJ, Beltz GE, Sun Y. In: Argon AS, editor. Topics in fracture and fatigue. New York: Springer; 1992.
[35] Young RJ. In: Pritchard G, editor. Developments in reinforced plastics-I. London: Applied Science; 1980. p. 257.
[36] Kinloch AJ, Young RJ. Fracture behavior of polymers. London: Elsevier; 1983.
[37] Williams JG. Fracture mechanics of polymers. New York: Wiley; 1984.
[38] Broutman LJ, McGarry FJ. Polym Engng Sci 1965;9:589.
[39] Broutman LJ, McGarry FJ. Polym Engng Sci 1965;9:609.
[40] Kramer EJ, Advances in polymer science, vol. 52/53. Berlin: Springer; 1983. p. 1.
[41] Kramer EJ, Berger LL, Advances in polymer science, vol. 91/92. Berlin: Springer; 1990. p. 1.
[42] Argon AS, Cohen RE, Advances in polymer science, vol. 91/92. Berlin: Springer; 1990. p. 301.
[43] Wellinghoff ST, Baer E. J Appl Polym Sci 1978;22:2025.

[44] Bucknall CB, Advances in polymer science, vol. 27. Berlin: Springer; 1978. p. 121.
[45] Dagli G, Argon AS, Cohen RE. Polymer 1995;36:2173.
[46] Tijssens MGA, van-der-Giessen E. Mech Mater 2000;32:19.
[47] Socrate S, Boyce MC, Lazzeri A. Mech Mater 2001;33:155.
[48] Gebizlioglu OS, Beckham HW, Argon AS, Cohen RE, Brown HR. Macromolecules 1990;23:3968.
[49] Brown HR, Argon AS, Cohen RE, Gebizlioglu OS, Kramer E. Macromolecules 1989;22:1002.
[50] Qin J, Argon AS, Cohen RE. J Appl Polym Sci 1999;71:2319.
[51] Piorkowska E, Argon AS, Cohen RE. Polymer 1993;34:4435.
[52] Argon AS, Cohen RE, Patel AC. Polymer 1999;40:6991.
[53] Sultan JN, McGarry FJ. Polym Engng Sci 1973;13:29.
[54] Sue H-J, Yee AF. Polym Engng Sci 1996;36:2320.
[55] Schwier CE, Argon AS, Cohen RE. Phil Mag 1985;52:581.
[56] Wu SJ. Polymer 1985;26:1855.
[57] Wu SJ. J Appl Polym Sci 1988;35:549.
[58] Muratoglu OK, Argon AS, Cohen RE. Polymer 1995;36:2143.
[59] Muratoglu OK, Argon AS, Cohen RE, Weinberg M. Polymer 1999; 40:2331.
[60] Borggreve RJM, Gaymans RJ. Polymer 1989;30:63.
[61] Dijkstra K, TerLaak J, Gaymans RJ. Polymer 1994;35:332.
[62] Borggreve RJM, Gaymams RJ, Schuijer J, Ingen-Housz JF. Polymer 1987;28:1489.
[63] Wilbrink MWL, Argon AS, Cohen RE, Weinberg M. Polymer 2001; 42:10155.
[64] Martuscelli E, Musto P, Ragosta G, editors. Advanced routes for polymer toughening. Amsterdam: Elsevier; 1996.
[65] Wu X, Zhu X, Qi Z. In: Proceedings of the Eighth International Conference on Deformation, Yield and Fracture of Polymers, vol. 78/ 1. London: The Plastics and Rubber Institute; 1991.
[66] (a) Thio YS, Argon AS, Cohen RE, Weinberg M. Polymer 2002;43: 3661. (b) Thio YS. PhD Thesis in Chem Engng. Mass Inst Technol; June 2003.
[67] Zuiderduin WCJ, Westzann C, Huetink J, Gaymans RJ. Polymer 2003;44:261.
[68] Bartczak Z, Argon AS, Cohen RE, Weinberg M. Polymer 1999;40: 2331.
[69] Bartczak Z, Argon AS, Cohen RE, Weinberg M. Polymer 1999;40: 2347.
[70] Kinloch AJ, Advances in polymer science, vol. 72. Berlin: Springer; 1985. p. 43.
[71] Argon AS. In: Salama K, Ravi-Chandar K, Taplin DMR, Rama Rao P, editors. Advances in fracture research, vol. 4. Oxford: Pergamon; 1989. p. 2661.
[72] Chow TS. J Polym Sci (Phys) 1978;16:959.
[73] Eshelby JD. Proc R Soc London, Ser A 1957;241:376.
[74] Danielsson M, Parks DM, Boyce MC. J Mech Phys Solids 2002;50: 351.
[75] Tzika PA, Boyce MC, Parks DM. J Mech Phys Solids 2000;48:1893.
[76] Edelson BI, Baldwin WM. Trans ASM 1962;55:230.
[77] Hutchinson JW. J Mech Phys Solids 1968;16:13. see also p. 337.
[78] Rice JR, Rosengreen GF. J Mech Phys Solids 1968;16:1.
[79] G'Sell C, Jonas JJ. J Mater Sci 1981;16:1956.
[80] Hartmann B, Jarzynski J. J Acoustic Soc Am 1974;74:1346.
[81] Tweed JH, Knott JF. Acta Metall 1987;35:1401.
[82] McCrum NG, Read BE, Williams G. Anelastic and dielectric effects in polymeric solids. New York: Dover; 1991.
[83] Koleski JV, Wartman LH. Poly(vinyl chloride). New York: Gordon & Breach; 1969.
[84] van Krevelen DW. Properties of polymers, 3rd ed. Amsterdam: Elsevier; 1997.
[85] Schmieder K, Wolf K. Kolloid Z 1953;134:149.
[86] Argon AS, Bartczak Z, Cohen RE, Muratoglu OK. In: Andersen SI, Brandsted P, Lilholt H, Lystrup Aa, Rheinlaender JT, Sorensen BF, Toftegaard M, editors. Polymeric composites—expanding the limits. Roskilde, Denmark: Riso, N.L.; 1997. p. 1.
[87] Bao G, Hutchinson JW, McMeeking RM. Acta Metall Mater 1991;39: 1871.